

# Chapter 2

## Overview of Vibration Energy Harvesting

### 2.1 Background of Energy Harvesting

The idea of extracting energy from ambient sources and accumulating and storing it for a useful purpose is called energy harvesting (EH). The idea of harvesting energy from ambient sources is not fresh, and its history dates back to the windmill and the waterwheel [1]. For many decades, researchers have been establishing techniques to harvest energy from heat and other ambient sources. However, owing to the low energy conversion efficiency and a higher power requirement by many electronic applications, the field of EH did not attract enough attention in the past.

With a global desire for harvesting ‘green energy’ from ambient sources and recent advances in low-powered portable wireless electronic devices, the area of EH has attained greater attention over the past few years. The drastic reduction in size and power utilisation of modern electronic devices has buoyant researchers and industry to discover schemes to implant an endless power supply means within these systems, which can harvest energy from their surroundings for their entire lifespan.

Conventionally, these low-powered systems are designed to function on limited electrochemical batteries, which need intermittent replacement (e.g. alkaline battery AA) or recharging (e.g. Nickel-Zinc, Nickel-Cadmium, Lithium-ion batteries). However, the advancement in conventional battery technology has not been rapid enough to fulfil the long-lasting power needs of these portable wireless electronic systems [1, 2]. Therefore, a periodic battery-recharging or substitution is an indispensable requirement for these electronic applications. In many applications, this is not a practical choice, e.g. battery-recharging where a standard power supply is unavailable in distant areas, or a battery-replacement in sensors implanted in giant structures or in implanted medical devices. Figure 2.1 illustrates advancements in the performance of laptop computers (a mobile technology example) on a logarithmic scale relative to a laptop from 1990 [1]. It can be seen from the graphs that the progress in battery energy express the slowest tendency in mobile

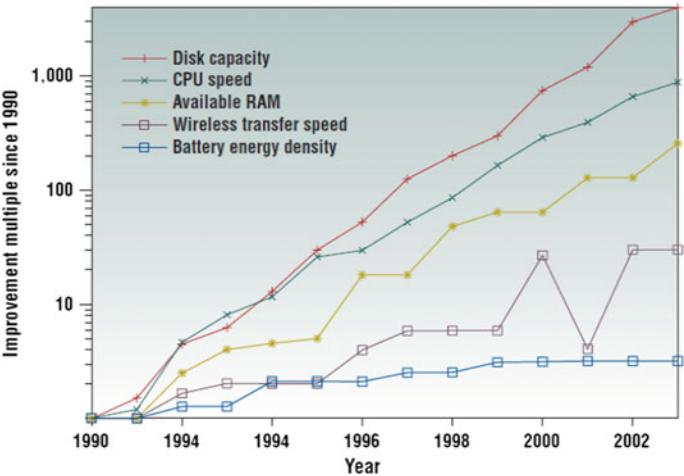


**Fig. 2.1** Relative advancements in processing and computing technology from 1990 to 2003 [1]

computing [1]. For these reasons, conventional batteries are no longer a rational energy resource in most modern electronic devices owing to the issues of recharging, replacement or disposal.

Tables 2.1 and 2.2 below present a short survey of specific power production capabilities of some common ambient energy sources together with the power consumption needs by some modern electronic devices. The power values in both tables are extracted from the published literature and are shown here for illustrative purposes only, as these values can be altered in different operating conditions. Thus, care should be taken in making comparative studies.

**Table 2.1** Electrical Power generation capacities of some ambient sources

Energy source	Conversion mechanism	Energy level	Reference
Vibration	Piezoelectric	100 mW/cm <sup>3</sup>	[2, 3]
	Electromagnetic	0.5–8 mW/cm <sup>3</sup>	[4]
	Electrostatic	8nW–42.9 μW/cm <sup>3</sup>	[5]
Light	Photovoltaic (solar)	100 mW/cm <sup>2</sup>	[6]
	Photovoltaic (indoor)	100 μW/cm <sup>2</sup>	
Ambient radiation	Radio frequency	≤ 1 mW/cm <sup>2</sup>	[1]
Wind	Turbine	200–800 μW/cm <sup>2</sup>	[5]
Thermal	Thermoelectric, thermionic, thermo-tunnelling	60 μW/cm <sup>2</sup>	[1]

**Table 2.2** Power utilisation by some portable wireless electronic devices

Electronic device	Power requirement	Reference
Electronic watch or calculator	1 $\mu$ W	[6]
Implanted medical devices	10 $\mu$ W	[7]
HTC Touch Pro phone (active mode) without GPS	29.1 $\mu$ W	[8]
Hearing aids	100 $\mu$ W	[6]
Hearing aids	1 mW	[7]
ET thermistor	3.5 mW	[9]
HTC Touch Pro phone (active mode) without GPS	24.8 mW	[8]
Bluetooth transceiver	45 mW	[6]
Palm MP3	100 mW	[6]
Phototransistor filter	150 mW	[10]

It can be observed from Tables 2.1 and 2.2 that the majority of the wireless electronic devices have the prospects of being powered by an implanted energy harvesting system in the near future.

## 2.2 Energy Harvesting from Vibrations

Williams and Yates [11] described three major vibration energy harvesting mechanisms: (1) electromagnetic, (2) electrostatic and (3) piezoelectric harvesting. In their research [11], Williams and Yates investigated the case of a lumped parameter base-excited model to analyse the electrical power generation for electromagnetic energy harvesting.

Electromagnetic energy harvesters are designed on the theory of Faraday's law of electromagnetic induction which describes that when a conductor (wire) is moved in a magnetic field, or vice versa, a voltage is generated around the conductor. The quantity of voltage produced by the electromagnetic induction is proportional to the rate of change of magnetic flux around the conductor. A classic electromagnetic energy harvester consists of a permanent magnet, a vibrating cantilever and a conducting coil as shown in Fig. 2.2 [12]. This technique does not require any outside power source to kick-start the energy harvesting process. However, the amount of energy harvested is proportional to the cube of the frequency of vibration [11], reducing its usefulness for low-frequency conditions. Moreover, the highest voltage generated by this transduction mechanism is usually quite low [13].

Electrostatic vibration energy conversion works on the rule of variable capacitance. The capacitance of a pre-charged capacitor changes as the distance between the two plates of a capacitor is varied. The charge on a capacitor is associated with the capacitance as:  $Q = CV$ , where  $Q$  is the charge on either plate,  $V$  is the voltage difference between the plates and  $C$  is the capacitance. The working principle of an

**Fig. 2.2** Schematic representation of a micro electromagnetic EH [12]

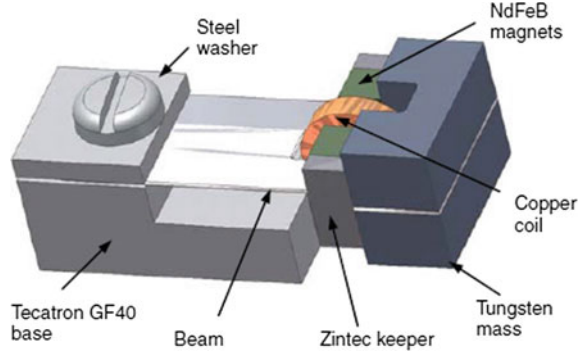
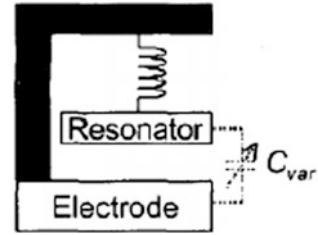


**Fig. 2.3** Working principle of an electrostatic vibration-based EH [14]



electrostatic energy harvester is shown in Fig. 2.3 [14]. By keeping either  $Q$  or  $V$  constant across an initially charged capacitor, any variation in  $C$  can cause variation in  $Q$  or  $V$ , which results in electrical charge production.

It is worth mentioning that the electrostatic vibration EH technique is not self-driven and requires an external power source to initially charge the capacitor and, thus, switch on the energy harvesting process. Moreover, the space available, within a capacitor itself, to allow the relative motion of the two capacitor plates is very narrow, which imposes durability hazards for the components.

Further details, elucidations and applications of electrostatic and electromagnetic vibration energy harvesting can be studied in references [11, 12, 14–18]. Table 2.1 illustrates that PVEH has a notably higher energy density level than both electromagnetic and electrostatic vibration EH techniques. For this basis and the other motives mentioned in Chap. 1, Sect. 1.1, this book is focused only on PVEH.

## 2.3 Piezoelectric Vibration Energy Harvesting (PVEH)

Previous research work broadly investigated the use of piezoelectric materials in vibration-to-electricity energy harvesters [2, 19–21]. To explore the ability of the piezoelectric energy harvesting technique from vibrations, researchers not only published different mathematical models but also provided experimental results

[22–25] to validate their proposed models. More generally, the research work in PVEH is mainly focused on:

- To develop mathematical techniques [26–34] to model the PVEH mechanism;
- To improve the geometrical and physical composition of harvesters [23, 35, 36] for maximising output;
- Enhancing the ability of electrical circuitry to extract more power [37–39];
- Studying the backward-coupling effects of piezoelectric energy harvesting on the dynamics of the system [27, 40–44];
- Improving the power storage medium [45, 46].

### 2.3.1 *Improvements in Modelling Techniques*

The modelling and analysis of the base-excited piezoelectric energy harvesting beams portrayed in Fig. 2.4 have fascinated many researchers with the aim of predicting the electrical output for given base motion input. In reference [22], it is illustrated that highly different modelling techniques had published in the literature during the preceding few years, and some of them might be ambiguous due to weak mathematical assumptions. For example, the early modelling attempt in reference [23] was based on a lumped parameter single degree of freedom (SDOF) model. Erturk and Inman [26, 28, 29] later showed that SDOF models for the distributed parameter systems in Fig. 2.4 may produce highly imprecise predictions. It was shown that, in the vicinity of the first natural frequency and without a tip mass, the errors in relative motion transmissibility functions when using a SDOF model can be greater than 35% irrespective of the mechanical damping [28]. Moreover, it was also presented that the error of using a SDOF model decreases as the ratio of tip mass to distributed mass of the beam is increased [28]. However, this technique (SDOF) continues to be used in theoretical studies, e.g. in reference [47].

A more exact approximation to the distributed parameter system has been acquired via the Rayleigh–Ritz type discrete formulation, e.g. [32]. This method uses a transformation of the displacements using appropriately selected basis functions. Hamilton’s Principle is then used to obtain discrete mass, stiffness and damping matrices in the transformed space. Analytical solutions that are limited to a single vibration mode expression have also been presented [48, 49]. Furthermore, these latter works have either ignored the essential effect of the piezoelectric coupling on the system dynamics [48] or oversimplified it as viscous damping [49]. Erturk and Inman [22] identify a more recent work [30] that is basically inconsistent since the piezoelectric effect is introduced on the basis of a static tip-force/deflection correlation.

A significant improvement in analytical modelling was made by Erturk and Inman [40], who applied an analytical modal analysis method (AMAM) to an Euler–Bernoulli model of a clamp-free uniform-section unimorph without tip mass. The piezoelectric coupling was precisely included through the piezoelectric

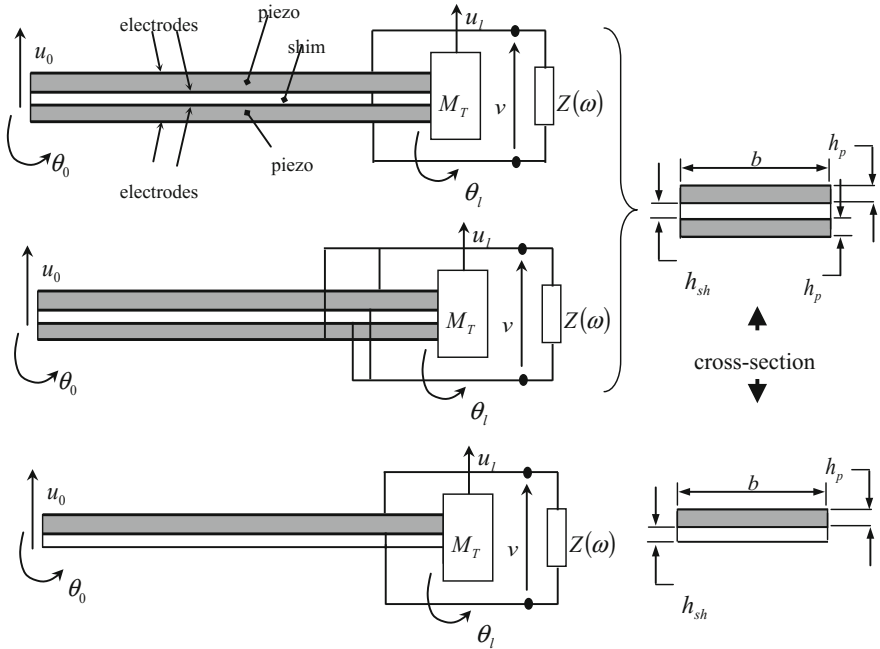


**Fig. 2.4** Base-excited piezoelectric EH beams (series-connected bimorph, upper figure; parallel-connected bimorph, middle figure; unimorph beam, lower figure)

constitutive relations. Terms accounting for material ('Kelvin-Voigt' or 'strain-rate') damping were included directly into the wave equation, in addition to ambient damping. The resultant wave equation with electromechanical coupling was transformed into modal space using the clamped-free bending modes of the undamped, electrically uncoupled beam. An analogous technique was later used in [22] to model a bimorph with a tip mass. Results for the frequency response functions (FRFs) relating the voltage and tip motion to the base excitation were illustrated in [22] over the first resonance region and experimentally validated. The presence of a tip mass in [22] reduced the influence of the distributed inertia of the beam and limited effective operation to low frequencies (e.g. 45–50 Hz resonance in [22]). A more rigorous experimental validation, covering the higher end of the frequency range of application, that most harvesters are designed for actual vibration conditions is necessary. This gap in the research is addressed in Chap. 3 of this book, which has been published in reference [25], and constitutes contribution no. 1 in Sect. 1.3.

None of the works in [22, 25, 40] validate their modelling over a wide frequency range against an alternative technique. However, Elvin and Elvin [50] presented that their numerical Rayleigh–Ritz (RR) solution converges to the AMAM solution [40] provided that appropriate basis functions are chosen for the RR method, and enough number of modes/basis functions are used in both methods. It is obvious

from the literature that PVEH beam modelling lacks an exact method that does not require approximations via modes/basis functions. This gap in the research is addressed in Chap. 4 of this book through the novel application of the dynamic stiffness method to PVEH beams [51–55]. The work in Chap. 4 has been published in reference [27] and contains contribution no. 2 in Sect. 1.3.

It is also worth mentioning that most of the distributed parameter modelling techniques, e.g. [22, 25, 29, 40] are based on a simple resistive impedance. Elvin and Elvin [50] stated that their model can entertain complex circuitry connected to the piezo but very little detail is presented in this regard. The work in this book addresses this gap in the research by generalising the analysis to generic resistor-capacitor-inductor circuitry.

### ***2.3.2 Progress in Geometric Configuration of Piezoelectric Harvester***

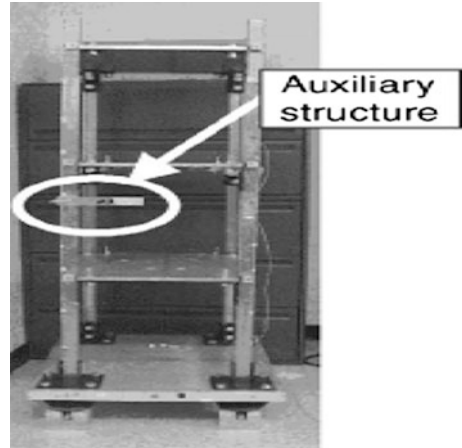
Previous research extensively investigated different piezoelectric energy harvesting configurations with the aim of increasing the power harvesting ability. The configuration of the PVEH device can be changed through diverse ways such as tuning the resonant frequency of the harvester; using multi-layers of the piezoelectric material to maximise the active volume; studying performance comparisons of various piezoelectric materials; changing the electrode pattern; changing the poling and stress direction; altering the coupling mode of the harvester; and optimising the geometrical shape of the device.

#### **2.3.2.1 Resonant Tuning the Harvester**

Most vibration-based piezoelectric energy harvesters produce peak power when the resonant frequency of the harvester matches with the frequency of the input ambient vibration. Any difference between these two frequencies can result in a considerable lessening in generated power. This is a basic disadvantage of piezoelectric resonant vibration energy harvesters which confines their power generation capability in real applications [47]. The aim of this section is to abridge the previous research investigating the resonance functionality of the harvester and its effects on power output. It is important to note that the contribution nos. 1, 2, 4 and 5 listed in Sect. 1.3, offer in-depth study of the power output of the PVEH system over a broad range of frequencies around the resonance.

The work [33] used an auxiliary structure which was tuned to the resonance frequency of the most dominant mode of vibration of three-storey host structure and connected it to the main structure. The auxiliary structure consisted of a mechanical fixture, a cantilever beam and a PZT element bonded on it as shown in Fig. 2.5.

**Fig. 2.5** Resonant Tuned auxiliary structure attached to a vibrating host structure [33]



A PZT bonded directly to the three-storey host structure generated 0.057 V, the PZT attached to the mistuned auxiliary structure produced 0.133 V and the PZT attached to the tuned auxiliary structure produced 0.335 V [33]. It is important to note that the PZT attached to a mistuned auxiliary structure produced twice more voltage output than the conventional technique of attaching it directly to the main host structure. The work in [33] only focussed on analysing the power outputs with and without the tuned auxiliary structure and did not study the alterations in the mechanical response of the host structure at the point of attachment.

The work [56] investigated the concept of active self-tuning of a piezoelectric generator to deal with the problem of mistuning of the harvester. The resonance frequency of the piezoelectric generator was harmonised with the resonance frequency of the ambient source by varying the effective stiffness or mass. Comparing to the extra power generated by adaptive tuning of the harvester with the power consumed by the tuning mechanism, the idea of self-active tuning did not prove efficiently in this approach [56].

A more effective method of achieving active self-tuning is through the addition of a microcontroller [57]. The microcontroller gets its power from the upper piezoelectric element of the bimorph, whereas the energy harvesting system is attached to the lower piezoelectric element of a bimorph as shown in Fig. 2.6.

The natural frequency of the power harvesting device was matched with the excitation frequency of the ambient vibration by changing the stiffness of the harvester beam [57], and a 30% average increase in harvested power was observed. The work stated that the major gains in the efficiency are achieved by reducing the structural stiffness and mechanical damping, and increasing the effective mass [57]. However, an inexact SDOF model was used to obtain the voltage equation, which is not an accurate selection as explained in Sect. 2.3.1. While the oversimplified model may be sufficient for preliminary power output study, it is not enough to study the effects of EH and its backward-coupling effects on the dynamics of the system.



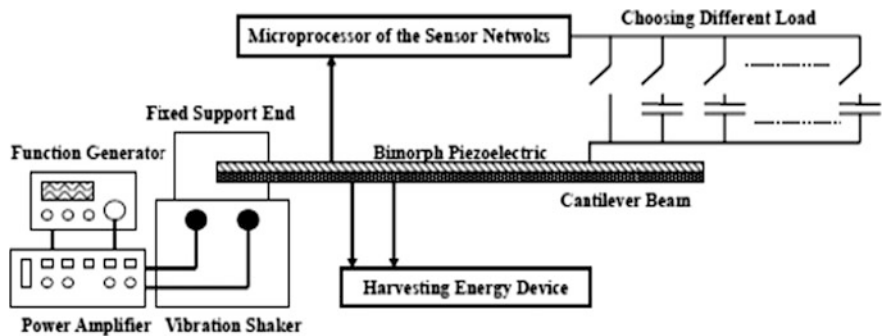


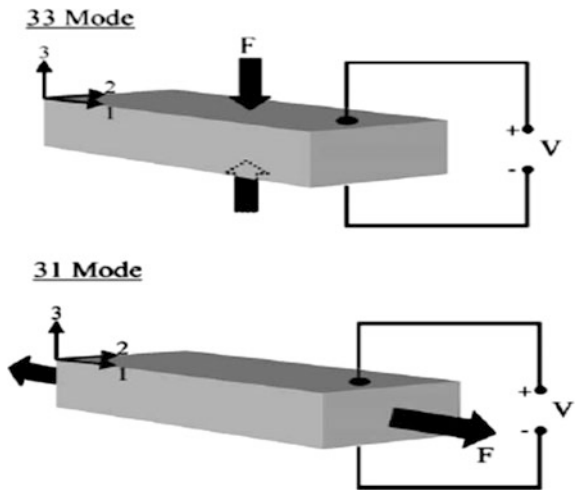
Fig. 2.6 Block diagram of experimental set-up of EH system [57]

2.3.2.2 Coupling Mode Effects on Power Output

The capability of a piezoelectric material to transform mechanical energy into electrical energy depends also on the piezoelectric coupling mode used in the energy harvesting system. Two practical piezoelectric coupling modes of operation exist, which are the  $-31$  mode and the  $-33$  mode as shown in Fig. 2.7 [23]. In  $-31$  mode, force is applied perpendicular to the poling direction, whereas in the  $-33$  mode the force is applied along the poling direction as shown in Fig. 2.7.

It is important to have proper consideration of piezoelectric mode of operation ( $-31$  or  $-33$ ) when designing a PVEH system since the power output and the dynamic properties of PVEH system fully depend on it. The  $-31$  mode has a lower coupling coefficient than the  $-33$  mode. The aim of this section is to investigate the performance of PVEH models in  $-31$  and  $-33$  modes as it is the main design feature with regard to the electromechanical conversion capacity of the harvester.

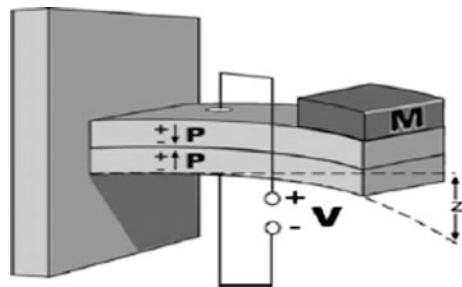
Fig. 2.7 Two piezoelectric coupling modes,  $-33$  mode and  $-31$  mode, loading operations [23]



The work [58] investigated a piezoelectric stack configuration in the  $-33$  mode, and the results were compared to the results from an equal volume of a cantilever beam operating in  $-31$  mode. The stiffer stack configuration was not an appropriate choice to create higher strain in the harvester for low-intensity ambient vibrations. Therefore, a lower electrical power output was achieved, even though the loading was applied in higher coupling mode ( $-33$  mode) [58]. On the other hand, the cantilever beam operating in  $-31$  mode (having lower coupling coefficient) produced twice as much power (compared to the stack configuration under the same loading conditions) [58]. This shows that in low-intensity vibration environment, a cantilever EH operating in  $-31$  mode is more efficient since it produces greater strain. For high-intensity vibration conditions, namely vibrations at the bases of manufacturing machinery, a stack configuration operating in  $-33$  mode is more useful and robust, and generates more power [58]. For these reasons, piezoelectric energy harvesters have been more yielding in  $-31$  coupling mode since more strains can be generated with smaller input forces [58]. Moreover, the resonant frequency of the system is much lesser in  $-31$  mode because of the reduced stiffness, thereby increasing the effectiveness of the EH system to operate at low ambient vibrations [23, 58]. Therefore, a clamp-free beam, with a tip mass at the free end as shown in Fig. 2.8, has been a useful PVEH configuration investigated by majority of researchers.

The rectangular clamp-free configuration is the most rigorously researched design in the PVEH literature. However, other designs have also been researched. For example, the works in [59, 60] examined analytically and experimentally the effectiveness of a membrane type geometry [60]. A lumped parameter model was used to study the effects of design and process parameters, such as residual stress, substrate thickness, piezoelectric thickness and electrode coverage, on the electromechanical *coupling coefficient* [60]. The work showed that the coupling coefficient and thereby the power output of the harvester enhanced considerably by the appropriate selection of residual stress, substrate thickness and the covered area of the electrodes in membrane harvester. It was observed that for a substrate of thickness  $2\text{ }\mu\text{m}$ , altering the thickness of piezoelectric layer from  $1$  to  $3\text{ }\mu\text{m}$ , increased the coupling coefficient 4 times. The experimental work presented that, for a membrane having an initial residual stress of  $80\text{ MPa}$ , the coupling coefficient was improved by  $150\%$  [59]. It should be noted that the work used a lumped

**Fig. 2.8** Functioning of a piezoelectric bimorph in a  $-31$  mode



parameter model to study the distributed parameter system which may yield highly inaccurate predictions as explained in Sect. 2.3.1.

### 2.3.2.3 Comparison of Various Piezo Materials and Shapes

A range of piezoelectric materials with a variety of electromechanical properties are easily available. The work in [35] explores the energy harvesting competences of three piezoelectric materials (Macro-fibre composites (MFC), quick pack (QP) and quick pack interdigitated electrodes (QP IDE)), attached to the same aluminium beam as shown in Fig. 2.9. In this method, all of the materials under consideration experienced the same input vibration excitation. The MFC contained piezoelectric fibres embedded in epoxy matrix that permitted greater flexibility and strain, and it utilised interdigitated electrode pattern which permitted the electric field to be applied along the length of the fibre, enabling it to function in a higher  $d_{33}$  coupling mode [35]. The work included the first 12 modes of the beam, and the amount of power harvested was recorded for all the materials.

The results illustrated that the quick pack showed to be more capable, extracting more power compared to MFC and quick pack IDE. It is important to note that the interdigitated electrode pattern of the MFC and quick pack decreased the capability of the devices to accumulate more charge and thereby reduced the net harvested power output. Furthermore, it was found in [35] that a high electromechanical coupling and permittivity values increases a material's ability to transfer more mechanical energy into electrical energy under given conditions. Moreover, the quantity of power produced by a brittle piezoelectric element may be smaller than the one produced by a flexible piezoelectric material. This may be due to the reason that the brittle materials can absorb less strain and hence produce a reduced power output. The work in [35] only compared the experimental power outputs of different

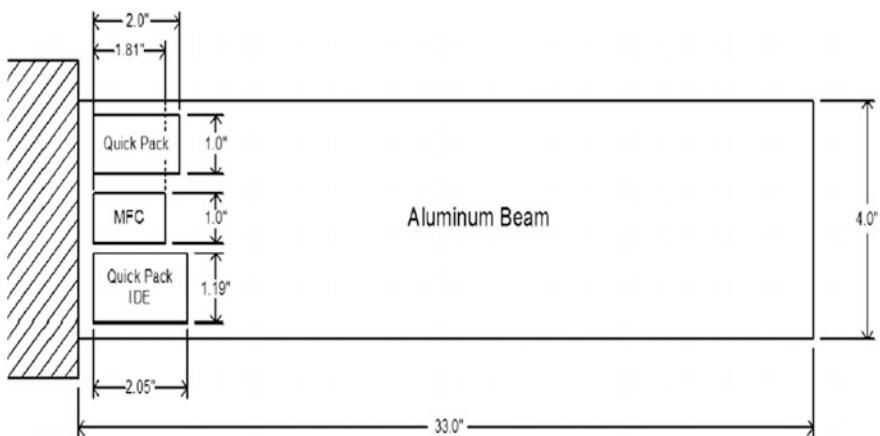
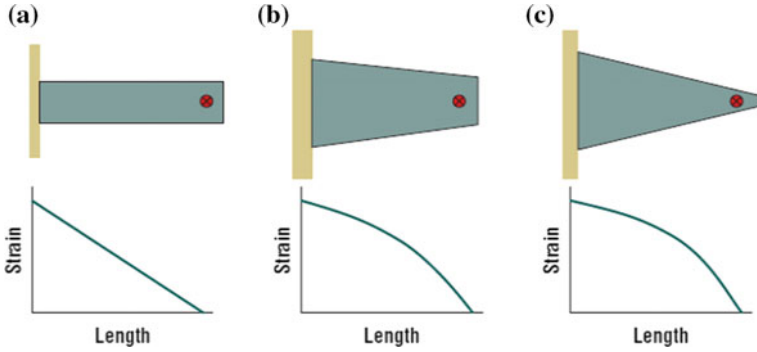


Fig. 2.9 QP, QP IDE, MFC patches bonded to same aluminium beam [35]



**Fig. 2.10** Relative bending energies and strain profiles for different beam configurations. Red circle indicates load point [3]

piezoelectric materials. The work neither used any mathematical model nor any other alternative theoretical method to evaluate and confirm the experimental results.

Typically, a rectangular cantilevered geometry has been a popular (e.g. uni-morphs or bi-morphs) option among the researchers working in PVEH. However, the work in reference [3] demonstrated that, with an increasingly trapezoidal-shaped cantilever, the strain distribution is consistently distributed all over the structure in comparison with a rectangular beam that contains a non-uniform strain distribution (Fig. 2.10). It was also shown that, for the same volume of PZT energy harvesters, a trapezoidal cantilever can generate more power than a rectangular beam [3].

In [61], the performance of various triangular- and rectangular-shaped beams, as shown in Fig. 2.11, was studied. It was demonstrated that the triangular-shaped beams performed better than the rectangular ones in terms of tolerable excitation amplitude and maximum power output [61].

In another study [62], different design configurations were studied to increase the specific power of the harvester by optimising its geometric shape. The power output for two trapezoidal-shaped harvesters (the wider side clamped or free) was compared with that of a conventional rectangular harvester. It was shown that the proposed optimised trapezoidal geometries produced more power output than the rectangular geometry, as can be seen in Fig. 2.12 [62].

To date, there are diverse piezoelectric materials and design configurations that are published in the literature with the definitive aim of maximising the output and thereby the efficiency of the energy harvesting system. Figure 2.13 shows examples of some generally available configurations of piezoelectric materials [19]. It is important to note that the work [3, 19, 61, 62] efficiently examines EH abilities of diverse harvester geometries to attain higher power but ignored the effects of energy harvester-host structure interaction in their models. These gaps in knowledge are addressed in this book (i.e. Chapter 4, 5, 6) through contributions nos. 6 and 7 listed in Sect. 1.3.

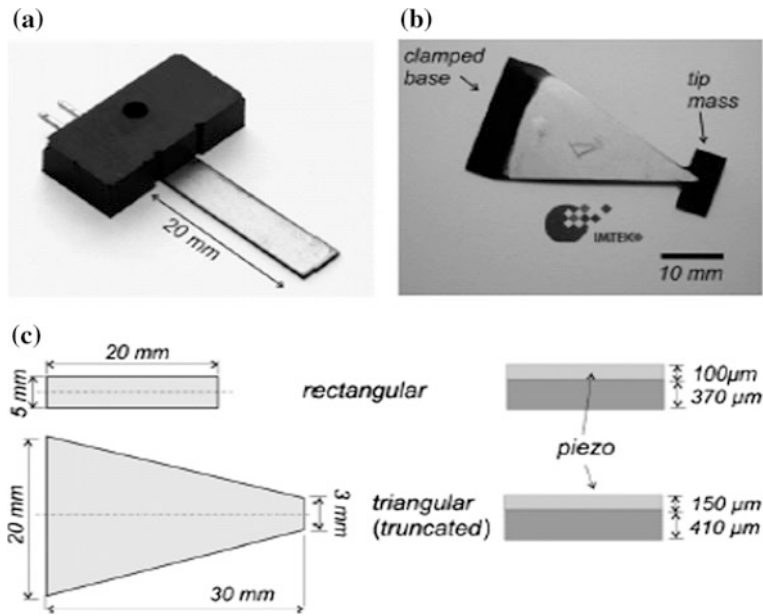
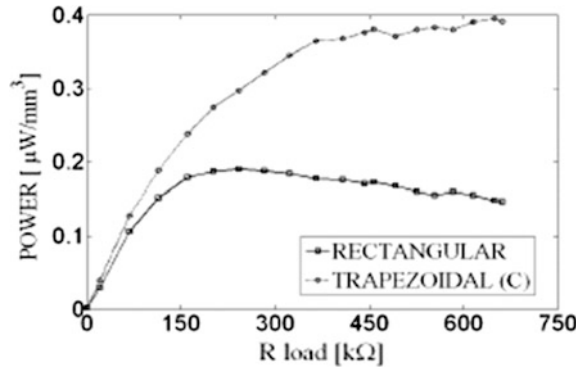


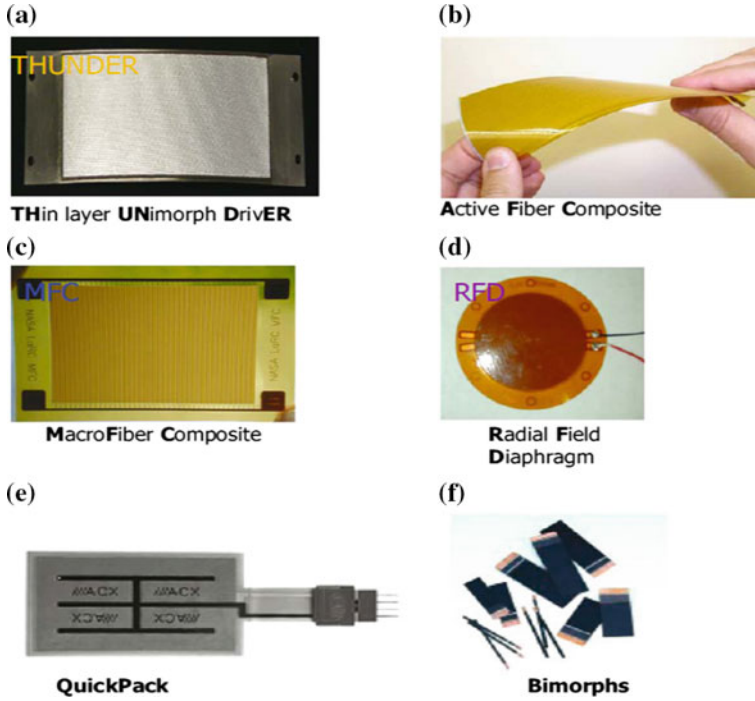
Fig. 2.11 Examples of different piezoelectric EH beam shapes [61]

Fig. 2.12 Comparison of power outputs of rectangular- and trapezoidal-shaped EH [62]



### 2.3.3 Application of PVEH in Vibration Control

Prior to considering the application of PVEH to vibration control, it is best to give a more general background to vibration control research, mainly tuned vibration absorbers. A tuned vibration absorber (TVA), in its most basic form, is an auxiliary system whose parameters can be tuned to suppress the vibration of a host structure. As discussed by von Flotow et al. [42], the auxiliary system is generally a structure that is equivalent to a spring-mass-damper system, in which case the TVA is



**Fig. 2.13** Examples of some piezoelectric energy harvester configurations [19]

referred to here as a ‘mechanical’ TVA. The tuned frequency  $\omega_a$  of the TVA is defined as its lowest undamped resonance frequency with its base (point of attachment) fixed. The mechanical TVA suppresses the vibration at its point of attachment to the host structure through the application of an interface force [63].

The TVA can be used in two distinct ways, resulting in different optimal tuning criteria and design requirements:

- It can be tuned to suppress the modal contribution from a specific troublesome natural frequency  $\Omega_s$  of the host structure over a wide band of excitation frequencies.
- It can be tuned to suppress the vibration at a specific troublesome excitation frequency, in which case it acts as a notch filter.

When used in application (b), a mechanical TVA is referred to as a tuned vibration neutraliser (or undamped TVA). In this case, the TVA is tuned to the excitation frequency, i.e. the condition  $\omega_a = \omega$  defines optimal tuning. In this condition, the neutraliser plants an anti-resonance at its point of attachment to the host structure, and the host vibration is suppressed over a very narrow bandwidth centred at  $\omega_a$ . In the absence of damping in the neutraliser, there is total attenuation of the vibration. The attenuation degrades with increasing absorber damping. In

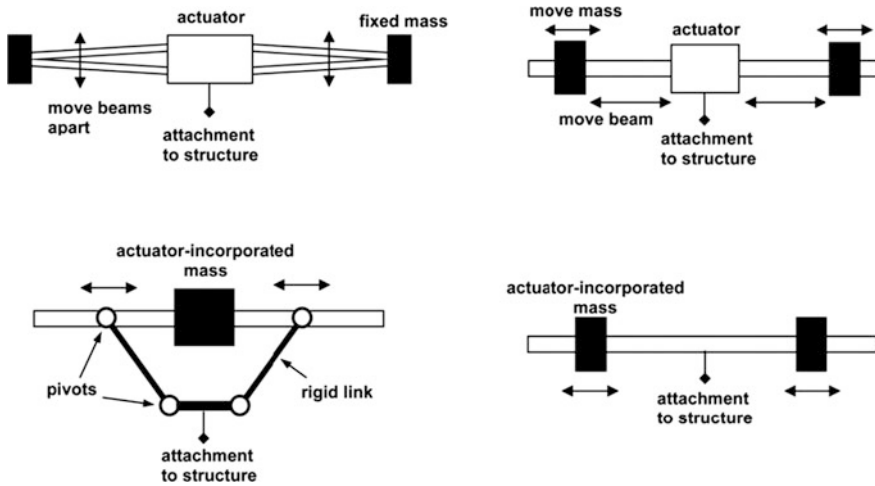


Fig. 2.14 Examples of adaptable beam type TVAs [64]

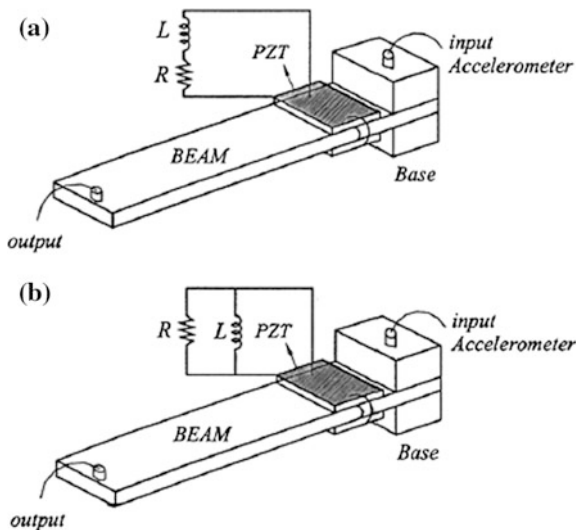
practice, a neutraliser can be conveniently implemented in the form of a simple beam-like structure [64], as shown in Fig. 2.14. Such beam-like configurations allow retuning of the device (adaptation) under variable conditions through the adjustment of the effective beam cross section or beam span. The method for the derivation of the equivalent two-degree-of-freedom model (minus the damping) for the beam structures in Fig. 2.14 was presented in [64].

When used in the application (a), a mechanical TVA is referred to as a tuned mass damper (TMD). In this case,  $\omega_a$  is tuned to a frequency that is slightly lower than that of the targeted vibration mode  $\Omega_s$ . A TMD needs the exact amount of optimal amount of damping in order to suppress the contribution of the targeted mode to the vibration frequency response at the point of attachment over a wide band of excitation frequencies. The practical implementation of the exact amount of damping in conventionally damped TMDs poses a design challenge. Furthermore, once implemented, such damping may be hard to adjust in response to varying system parameters. Moreover, the prerequisite for damping means that simple beam-like designs (Fig. 2.14) are complex to realise for TMDs.

As mentioned by von Flotow [42], a TVA can also be realised with other physics. The most relevant in the present context is the ‘electrical’ TVA [41], which is normally used for application (a) discussed above (i.e. analogous to the TMD). In such a device, the auxiliary system is a piezoelectric shunt circuit. A piezoelectric patch is attached directly to the host structure (typically a cantilever beam) and connected across an external inductor-resistor circuit, as shown in Fig. 2.15 [41].

The piezoelectric patch is used to transfer the vibration energy of the host structure into electrical energy and added a capacitor effect into the circuit, turning it into an R-L-C circuit. The electrical energy is then dissipated most efficiently as Joule heating through the resistor when the electrical resonance produced by the

**Fig. 2.15** **a** An ‘electrical’ TVA attached to host structure (cantilever beam) with series R-L and **b** with parallel R-L [41]



L-C components is close to the frequency of the targeted mode. An optimal resistance value provides that the contribution of the targeted mode to the vibration frequency response at a chosen location is suppressed over a wide band of excitation frequencies.

The work in [65] investigated the use of such an electrical TVA (i.e. shunted piezo patch bonded to a host structure whose vibration is to be controlled) for various types of electrical circuits: (1) resistive shunt which dissipates energy and works as a damper, (2) an inductive shunt which results in resonant L-C circuit, (3) a capacitive shunt that changes the stiffness of the piezoelectric element and (4) a switched shunt that controls the energy transfer [65]. In [44, 65–67], the electrical damping effects added by the piezo patch to the system to which it is bonded are analysed. To estimate the electrical damping, the resonance frequency and the damping of the fundamental vibration mode were measured at open circuit, short circuit and when the energy harvesting system was in operation [44]. For the case studied, the mechanical coupling coefficient of the system and the mechanical loss factor were calculated as 0.264 and 2.3%, respectively [44]. In [66], a model was developed and the amount of electrical energy generated by vibrating piezoelectric patches was predicted. The work in [66] presented a relatively simple approach of visualising the electrical damping effects through the comparison of the impulse response of a cantilever beam for very low load, an optimum load (yielding maximum power), and a very high load. The comparison of the three graphs indicated a considerable rise in damping of the system which can be noted from the settling time shown in Fig. 2.16. Similar illustrations and studies investigating the electrical shunt damping effects on the structural response are discussed in references [68–72].



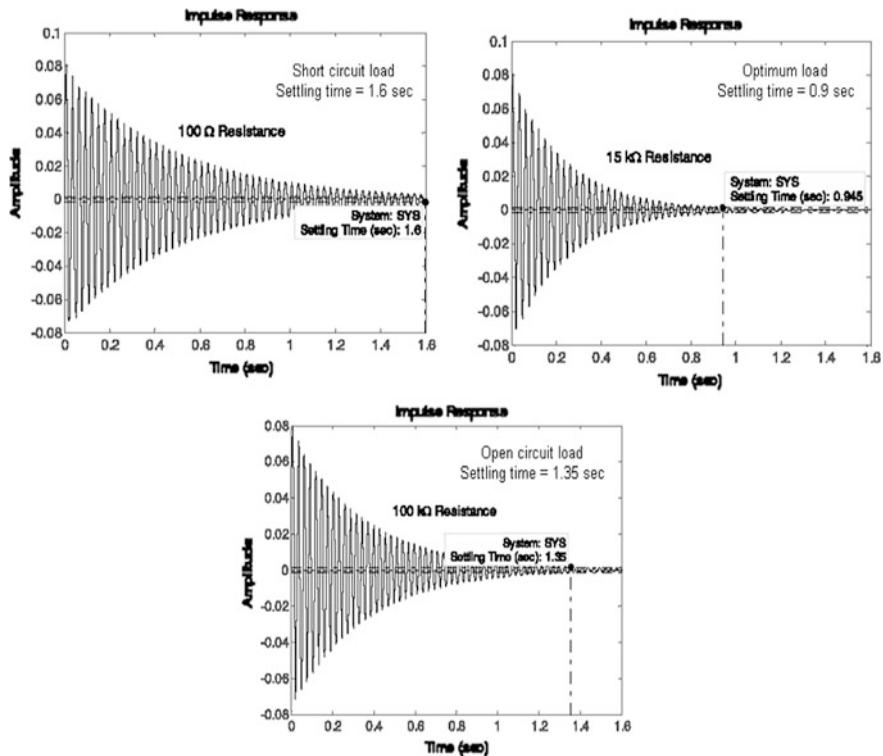


Fig. 2.16 Comparison of damping at different loads [66]

Relative to conventional viscoelastic material damping treatments that can be applied to beams, the electrical TVA has the following advantages: (a) robustness and compactness; (b) relatively less temperature dependence; and (c) ease of controlling the damping level for the desired vibration suppression [41, 68, 72, 73]. These advantages also apply when comparing the electrical TVA to the conventional TMD, which is also limited by space constraints due to its larger size. However, the analysis required to predict the optimal parameters of the electrical TVA are not tractable to complex generic host structures. Such analysis involves the setting up of the coupled electromechanical equations of the host structure with the shunted piezo patch attached and their transformation to modal space, in much the same way as the AMAM analysis (Chap. 3 of this book). The transfer function governing the modal vibration at a specified location could then be extracted and optimised [41]. For this reason, the electrical TVA has only been analysed and presented for the simplest of host structures, namely the cantilever beams in Fig. 2.15 [41]. In contrast, the conventional theory of the classic TMD is readily

applicable to any arbitrary host structure since the only host structure data needs are the frequency  $\Omega_s$  and mass  $M_A^{(s)}$  of the targeted mode. The relative shortcomings of the mechanical TVA and electrical TVA are overcome through contribution no. 7 listed in Sect. 1.3 and presented in Chaps. 5 and 6, wherein a dual EH/TVA beam or ‘electromechanical’ TVA is introduced.

### 2.3.4 Application of PVEH in Nanogenerators

The PVEH systems can also have enormous applications in nanotechnology devices [74]. It is found from current advancements in the fabrication of PZT nanofibers that such nanofibers may have an even superior piezoelectric voltage constant, higher bending flexibility and larger mechanical strength than bulk PZT which would support its use in nanogenerators [74]. Owing to these properties of PZT nanofibers, it would likely to generate higher voltages and power outputs than other types of piezoelectric geometric configurations for a given volume and same input vibration energy source. Therefore, the properties of PZT nanofibers have introduced considerable interest in taking benefit of these nanofibers in the development of nanogenerators. It is worth mentioning that, although, the concept of harvesting vibration energy by application of nanofiber piezo materials have shown noteworthy improvements, still there is enormous prospects exist for further research to facilitate the development of nanowire-based generators for future miniature applications [74].

## 2.4 Chapter Summary

This chapter has presented a broad review on PVEH as well as its application to vibration control. It started by giving a brief background of energy harvesting and its necessity for potential applications. This was then followed by a critical review of vibration-based energy harvesting with focus on PVEH modelling techniques. Previous research relating to the improvements in the piezoelectric energy harvester configurations was then reviewed in detail. Finally, research into the electromechanical coupling effects of PVEH on the dynamics of the system was discussed. The shortcomings and gaps in the research were highlighted at different stages in this review in order to explain the drive for the various novel contributions listed in Sect. 1.3.

## References

1. Paradiso, J., & Starner, T. (2005). Energy scavenging for mobile and wireless electronics. *IEEE Pervasive Computing*, 4(1), 18–27.
2. Anton, S. R., & Sodano, H. A. (2007). A review of power harvesting using piezoelectric materials (2003–2006). *Smart Materials and Structures*, 16(3), R1–R21.
3. Roundy, S., Leland, E. S., Baker, J., Carleton, E., Reilly, E., Lai, E., et al. (2005). Improving power output for vibration-based energy scavengers. *IEEE Pervasive Computing*, 4(1), 28–36.
4. Cook-Chennault, K. A., Thambi, N., & Sastry, A. M. (2008). Powering MEMS portable devices—A review of non-regenerative and regenerative power supply systems with special emphasis on piezoelectric energy harvesting systems. *Smart Materials & Structures*, 17(4).
5. Knight, C., Davidson, J., & Behrens, S. (2008). Energy options for wireless sensor nodes. *Sensors*, 8(12), 8037–8066.
6. Harrop, P., & Das, R. (2009). *Energy harvesting and storage for electronic devices 2009-2019* (p. 333) (IDTechEx report).
7. Raju, M., & Grazier, M. (2010). *Energy harvesting ULP meets energy harvesting: A game-changing combination for design engineers* (p. 8). Dallas, Texas: Texas Instruments.
8. Priyantha, B. L., Lymberopoulos, D., & Liu, J. (2010). *Energy efficient responsive sleeping on mobile phones*. Redmond, WA 98052: Microsoft Research.
9. Semitec, A. (2011). [cited 2011 07 July]. Thermal controls to the electrical and electronics industries. <http://www.atcsemitec.co.uk>.
10. Farnell. (2011). [cited 2011 July]. <http://www.uk.farnell.com>.
11. Williams, C. B., & Yates, R. B. (1996). Analysis of a micro-electric generator for microsystems. *Sensors and Actuators, A: Physical*, 52(1–3), 8–11.
12. Beeby, S. P., Torah, R. N., Tudor, M. J., Glynne-Jones, P., Saha, C. R., O'Donnell, T., et al. (2007). A micro electromagnetic generator for vibration energy harvesting. *Journal of Micromechanics and Microengineering*, 17(7), 1257–1265.
13. Roundy, S., Wright, P. K., & Rabaey, J. (2003). A study of low level vibrations as a power source for wireless sensor nodes. *Computer Communications*, 26(11), 1131–1144.
14. Miyazaki, M., Tanaka, H., Ono, G., Nagano, T., Ohkubo, N., Kawahara, T., & Yano, K. (2003). Electric-energy generation using variable-capacitive resonator for power-free LSI: Efficiency analysis and fundamental experiment. In *International Symposium on Low Power Electronics and Design*.
15. Beeby, S. P., Tudor, M. J., & White, N. M. (2006). Energy harvesting vibration sources for microsystems applications. *Measurement Science & Technology*, 17, 175–195.
16. Galayko, D., Guillemet, R., Dudka, A., & Basset, P. (2011). Comprehensive dynamic and stability analysis of electrostatic vibration energy harvester (E-VEH). In *Solid-State Sensors Actuators and Microsystems Conference (TRANSDUCERS)* (pp. 2382–2385).
17. Sidek, O., Khalid, M. A., Ishak, M. Z., & Miskam, M. A. (2011). Design and simulation of SOI-MEMS electrostatic vibration energy harvester for micro power generation. In *Electrical, Control and Computer Engineering (INECCE)* (pp. 207–212).
18. Dayal, R., & Parsa, L. (2011). Low power implementation of maximum energy harvesting scheme for vibration-based electromagnetic microgenerators. *IEEE Applied Power Electronics Conference and Exposition—APEC*.
19. Priya, S. (2007). Advances in energy harvesting using low profile piezoelectric transducers. *Journal of Electroceramics*, 19(1), 165–182.
20. Du, S., Jia, Y., & Seshia A., (2016). Piezoelectric vibration energy harvesting: A connection configuration scheme to increase operational range and output power. *Journal of Intelligent Material Systems and Structures*, 28(14), 1905–1915.
21. Kundu, S., & Nemade, H. B. (2016). Modeling and simulation of a piezoelectric vibration energy harvester. *Procedia Engineering*, 144, 568–575.

22. Erturk, A., & Inman, D. J. (2009). An experimentally validated bimorph cantilever model for piezoelectric energy harvesting from base excitations. *Smart Materials and Structures*, 18(2), 025009–025009.
23. Roundy, S., Paul K. W., & Rabaey, J. M. (2004). *Energy scavenging for wireless sensor networks with special focus on vibrations* (1st ed.). Kluwer: Kluwer Academic Publishers.
24. DuToit, N., & Wardle, L. (2007). Experimental verification of models for microfabricated piezoelectric vibration energy harvesters. *AIAA Journal*, 45(5), 1126–1137.
25. Rafique, S., & Bonello, P. (2010). Experimental validation of a distributed parameter piezoelectric bimorph cantilever energy harvester. *Smart materials and structures*, 19(9).
26. Erturk, A., & Inman, D. J. (2008). Issues in mathematical modeling of piezoelectric energy harvesters. *Smart materials & structures*, 17(6).
27. Bonello, P., & Rafique, S. (2011). Modeling and analysis of piezoelectric energy harvesting beams using the dynamic stiffness and analytical modal analysis methods. *Journal of Vibration and Acoustics*, 133(1), 011009.
28. Erturk, A., & Inman, D. J. (2008). Mechanical considerations for modeling of vibration-based energy harvesters. In *Proceedings of the ASME International Design Engineering Technical Conferences and Computers and Information in Engineering Conference*.
29. Erturk, A., & Inman, D. J. (2008). On mechanical modeling of cantilevered piezoelectric vibration energy harvesters. *Journal of Intelligent Material Systems and Structures*, 19(11), 1311–1325.
30. Ajitsaria, J., Choea, S., Kimb, D., & Shenb, D. (2007). Modeling of bimorph piezoelectric cantilever beam for voltage generation. In *Sensors and Smart Structures Technologies for Civil, Mechanical, and Aerospace Systems 2007*. San Diego, California: SPIE.
31. Roundy, S. (2005). On the effectiveness of vibration-based energy harvesting. *Journal of Intelligent Material Systems and Structures*, 16(10), 809–823.
32. Sodano, H. A., Park, G., & Inman, D. J. (2004). Estimation of electric charge output for piezoelectric energy harvesting. *Strain*, 40(2), 49–58.
33. Cornwell, P. J., Goethal, J., & Kowko, J. (2005). Enhancing power harvesting using a tuned auxiliary structure. *Journal of Intelligent Material Systems and Structures*, 16(10), 825–834.
34. DuToit, N., Wardle, L. W., & Kim, S. (2005). Design considerations for MEMS-scale piezoelectric mechanical vibration energy harvesters. *Integrated ferroelectrics*, 71, 121–160.
35. Sodano, H. A., Lloyd, J., & Inman, D. J. (2006). An experimental comparison between several active composite actuators for power generation. *Smart Materials and Structures*, 15(5), 1211–1216.
36. Shu, Y. C., & Lien, I. C. (2006). Analysis of power output for piezoelectric energy harvesting systems. *Smart Materials and Structures*, (6).
37. Ng, T. H., & Liao, W. H. (2004). Feasibility study of a self-powered piezoelectric sensor. *Proceedings of SPIE—The International Society for Optical Engineering*, 5389, 377–388.
38. Han, J., Annette, V. H., Triet, L. Mayaram, K., & Fiez, T. (2004). Novel power conditioning circuits for piezoelectric micropower generators IEEE. In *Applied Power Electronics Conference & Exhibition (APEC)*.
39. Ottman, G. K., Hofmann, H. F., & Lesieutre, G. A. (2003). Optimized piezoelectric energy harvesting circuit using step-down converter in discontinuous conduction mode. *IEEE Transactions on Power Electronics*, 18(2), 696–703.
40. Erturk, A., & Inman, D. J. (2008). Distributed parameter electromechanical model for cantilevered piezoelectric energy harvesters. *Journal of Vibration and Acoustics*, 130(4), 041002–041002.
41. Park, C. H. (2003). Dynamics modelling of beams with shunted piezoelectric elements. *Journal of Sound and Vibration*, 268(1), 115–129.
42. Flotow, V. B., & Bailey, D. (1994). Adaptive tuned vibration absorbers: Tuning laws, tracking agility, sizing, and physical implementations. In *Proceedings of National Conference on Noise Control Engineering. Progress in Noise Control for Industry*.
43. Sodano, H. A., Inman, D. J., & Park, G. (2004). A review of power harvesting from vibration using piezoelectric materials. *The Shock and Vibration Digest*, 36(3), 197–205.

44. Lesieutre, G. A., Ottman, G. K., & Hofmann, H. F. (2004). Damping as a result of piezoelectric energy harvesting. *Journal of Sound and Vibration*, 269(3), 991–1001.
45. Sodano, H. A., & Inman, D. J. (2005). Generation and storage of electricity from power harvesting devices. *Journal of Intelligent Material Systems and Structures*, 16(1), 67–75.
46. Sodano, H. A., Inman, D. J., & Park, G. H. (2005). Comparison of piezoelectric energy harvesting devices for recharging batteries. *Journal of Intelligent Material Systems and Structures*, 16(10), 799–807.
47. Zhu, D., Tudor, M. J., & Beeby, S. P. (2010). Strategies for increasing the operating frequency range of vibration energy harvesters: A review. *Measurement science & technology*, 21(2).
48. Lu, F. (2004). Modeling and analysis of micro piezoelectric power generators for micro-electromechanical-systems applications. *Smart Materials and Structures*, 13(1), 57–63.
49. Chen, S., Wang, G., & Chien, M. (2006). Analytical modeling of piezoelectric vibration-induced micro power generator. *Mechatronics*, 16(7), 379–387.
50. Elvin, N. G., & Elvin, A. A. (2009). A general equivalent circuit model for piezoelectric generators. *Journal of Intelligent Material Systems and Structures*, 20(1), 3–9.
51. Chen, Y. H., & Sheu, J-Ts. (1996). Beam length and dynamic stiffness. *Computer Methods in Applied Mechanics and Engineering*, 129(3), 311–318.
52. Eisenberger, M. (1995). Dynamic stiffness matrix for variable cross-section Timoshenko beams. *Communications in Numerical Methods in Engineering*, 11(6), 507–513.
53. Henshell, R. D., & Warburton, G. B. (1969). Transmission of vibration in beam systems. *International Journal for Numerical Methods in Engineering*, 1(1), 47–66.
54. Chen, Y. H. (1987). General dynamic stiffness matrix of a Timoshenko beam for transverse vibrations. *Earthquake Engineering and Structural Dynamics*, 15, 391–402.
55. Roundy, S., & Zhang, Y. (2005). Toward self-tuning adaptive vibration-based microgenerators. *Proceedings of SPIE—The International Society for Optical Engineering*, 5649(1), 373–384.
56. Wu, W.-J., Chen, Y., Lee, B., He, J., & Peng, Y. (2006). Tunable resonant frequency power harvesting devices. *Proceedings of SPIE—The International Society for Optical Engineering*, 6169, 61690–61690.
57. Bonello, P., & Brennan, J. (2001). Modelling the dynamic behaviour of a supercritical rotor on a flexible foundation using the mechanical impedance technique. *Journal of Sound and Vibration*, 239(3), 445–466.
58. Baker, J., Roundy, S., & Wright, P. (2005). Alternative geometries for increasing power density in vibration energy scavenging for wireless sensor networks. In *Collection of Technical Papers—3rd International Energy Conversion Engineering Conference*.
59. Cho, J., Anderson, M., Richards, R., Bahr, D., & Richards, C. (2005). Optimization of electromechanical coupling for a thin-film PZT membrane: II. Experiment. *Journal of micromechanics and microengineering*, 15(10), 1804–1809.
60. Cho, J., Anderson, M., Richards, R., Bahr, D., & Richards, C. (2005). Optimization of electromechanical coupling for a thin-film PZT membrane: I. Modeling. *15(10)*, 1797–1803.
61. Goldschmidtboeing, F., & Woias, P. (2008). Characterization of different beam shapes for piezoelectric energy harvesting. *Micromechanics and Microengineering*, 18.
62. Brusa, E., Zelenika, S., Morob, L., & Benasciuttib, D. (2009). Analytical characterization and experimental validation of performances of piezoelectric vibration energy scavengers. *Proceedings of SPIE—The International Society for Optical Engineering*, 7362.
63. Kidner, M., & Brennan, M. J. (1999). Improving the performance of a vibration neutraliser by actively removing damping. *Journal of Sound and Vibration*, 221(4), 587–606.
64. Bonello, P., & Groves K. H. (2009). Vibration control using a beam-like adaptive tuned vibration absorber with an actuator-incorporated mass element. *Mechanical Engineering Science*, 223(7).
65. Lesieutre, G. (1998). Vibration damping and control using shunted piezoelectric materials. *The Shock and Vibration Digest*, 30(3), 187–195.

66. Sodano, H. (2003). Model of piezoelectric power harvesting beam. In *Proceedings of the ASME Aerospace Division—2003, AD*.
67. Yabin, L., & Henry, A. S. (2010). Piezoelectric damping of resistively shunted beams and optimal parameters for maximum damping. *Journal of Vibration and Acoustics*, 132(4), 041014.
68. Hagood, N. W., & Von Flotow, A. (1991). Damping of structural vibrations with piezoelectric materials and passive electrical networks. *Journal of Sound and Vibration*, 146(2), 243–268.
69. Davis, C. L., & Lesieutre, G. A. (1995). A modal strain energy approach to the prediction of resistively shunted piezoceramic damping. *Journal of Sound and Vibration*, 184(1), 129–139.
70. Fleming, A. J., Behrens, S., & Moheimani, S. O. R. (2001). Innovations in piezoelectric shunt damping. In *Smart Structures and Devices, Proceedings of SPIE*.
71. Liang, J. R. (2009). Piezoelectric energy harvesting and dissipation on structural damping. *Journal of Intelligent Material Systems and Structures*, 20(5), 515–527.
72. Hollkamp, J., & Starchville, T. F. (1994). Self-tuning piezoelectric vibration absorber. *Journal of Intelligent Material Systems and Structures*, 5(4), 559–566.
73. Law, H. H. (1996). Characterization of mechanical vibration damping by piezoelectric materials. *Journal of Sound and Vibration*, 197(4), 489–513.
74. Shiyu, X., Yong, S., & Sang-Gook, K. (2006). Fabrication and mechanical property of nano piezoelectric fibres. *Nanotechnology*, 17(17), 4497.

**Piezoelectric Vibration Energy Harvesting**

**Modeling & Experiments**

Rafique, S.

2018, XVIII, 172 p. 87 illus., 41 illus. in color., Hardcover

ISBN: 978-3-319-69440-5